

Synthesis, Structure and Chemistry of a Twisted Olefinic Bis-didentate Proligand: 5,5'-Bi-5*H*-cyclopenta[2,1-*b*:3,4-*b'*]dipyridinylidene

by Marianne Riklin and Alexander von Zelewsky

Institute of Inorganic Chemistry, University of Fribourg, Perolles, CH-1700 Fribourg

and Alan Bashall and Mary McPartlin

School of Biological and Applied Sciences, University of North London, Holloway Road, London N7 8DB, U.K.

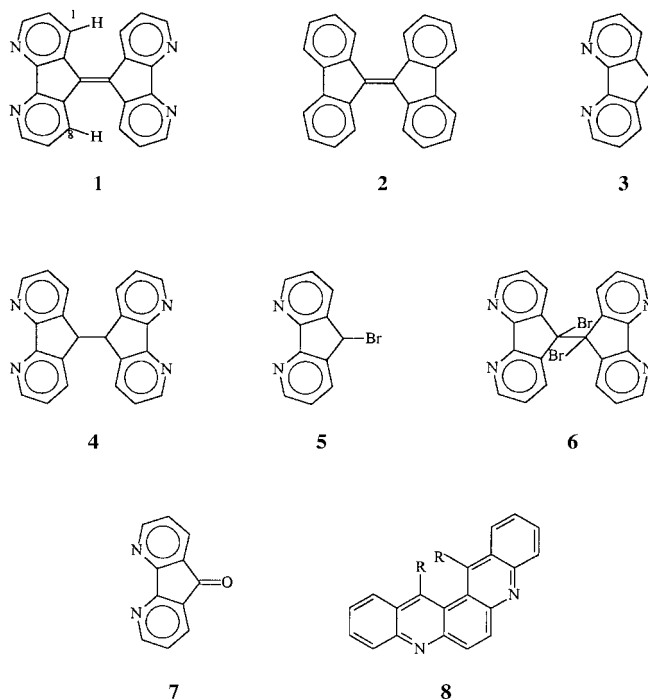
and Akin Baysal, Joseph A. Connor*¹⁾ and John D. Wallis

Chemistry Department, School of Physical Sciences, University of Kent, Canterbury, Kent, CT2 7NR, U.K.

The elusive chiral twisted alkene, 5,5'-bi-5*H*-cyclopenta[2,1-*b*:3,4-*b'*]dipyridinylidene, known also as 9,9'-bi-4,5-diazafluorenylidene (BDAF), has been prepared in racemic form from 9-bromo-4,5-diazafluorene and from 9,9'-bi-4,5-diazafluorenyl and fully characterised. X-Ray measurements show that there is a twist of 37.8° about the double bond between the 4,5-diazafluorenylidene units. A 1:1 charge-transfer compound with 7,7,8,8-tetracyanoquinodimethane (TCNQ) contains an unusual packing arrangement which is centred around the formation of spiral stacks. Each BDAF molecule contributes one 4,5-diazafluorenylidene unit to the backbone of the stack, while the second half is involved in hydrogen-bonding interactions and additional stacking with TCNQ. Examples of complexes containing the axially symmetric tetradentate ligand binding to one and to two metal ions, $[M(\text{bdaf})\text{Cl}_2]$ and $[(M\text{Cl}_2)_2(\text{bdaf})]$ ($M = \text{Co}, \text{Ni}, \text{Zn}$), are reported.

Introduction. – The intramolecular energy- and electron-transfer properties of supramolecular assemblies [1] formed by dendrimeric complexes such as $[\text{Ru}\{\{\mu\text{-dpp}\}\text{Ru}\{\{\mu\text{-dpp}\}\text{Ru}(\text{bpy})_2\}_2\}_3]^{4+}$ (dpp = 2,3-di(2-pyridyl)pyrazine [2]) have attracted much attention recently [3]. The role of the tetradentate bridging ligand in such complexes is crucial. The range of suitable pro-ligands [4] is limited, and difficult stereochemical problems are presented by these polymetallic complexes. To avoid the formation of geometric isomers (*fac*, *mer*), the tetradentate bridging ligand should be symmetric with respect to the axis of coordination. This requirement is fulfilled by 2,2'-bipyrimidine (bpym) [5], and by 9,9'-bi-4,5-diazafluorenylidene (bdaf) [6] (**1**), for example. In the course of work [7] on the oxidation of 4,5-diazaphenanthrene, we noticed a description of **1** as a colorless crystalline solid [8]. This observation was remarkable, because it has long been known that the hydrocarbon 9,9'-bifluorenylidene (**2**) is a bright red solid [9], the structure of which [10] is not planar. We set out to repeat the published [8] preparation of **1**, but despite much effort we were unsuccessful. The products were easily identified as 4,5-diazafluorene (**3**) [11] and 9,9'-bi-4,5-diazafluorenyl (**4**) [12]. Consequently, we have devised other simple approaches to **1**.

¹⁾ Fax: +44 1227 827724; e-mail: j.a.connor@ukc.ac.uk.



Results and Discussion. – Bromination of **3** using 1 equiv. of *N*-bromosuccinimide (NBS) in benzene [13] gave two products, 9-bromo-4,5-diaza-9*H*-fluorene (**5**; 60% yield), and 9,9'-bi-9-bromo-4,5-diaza-9*H*-fluorenyl (**6**; 20% yield). Dehydrobromination of **5** with *t*-BuOK/*t*-BuOH [14] gave **1** (90% yield) as an orange powder. A second approach involved dehydrogenation of 9,9'-bi-4,5-diaza-9*H*-fluorenyl (**4**), the minor (40% yield) product of the *Wolff-Kishner* reduction of 4,5-diaza-9*H*-fluorene-9-one [12] (**7**) with 2,3-dichloro-5,6-dicyano-1,4-benzoquinone (DDQ) [15] in PhBr. The oxidation is fast and leads to a good yield (85%) of **1**. Alternatively, reaction of **4** with NBS in the presence of a catalytic quantity of dibenzoyl peroxide in CHCl₃ [16] also produces **1** in good yield (86%). The orange solid **1** does not melt below 593 K; it is slightly soluble in benzene and is readily soluble in polar solvents such as CHCl₃ and MeCN. The mass spectrum shows an intense molecular ion (*m/z* 332). The temperature-independent (200–400 K) ¹H- and ¹³C-NMR parameters are shown in *Table 1*, which also contains comparable data for **2**, **3**, **4** and **7**. It is particularly noteworthy that the protons H–C(1) and H–C(8), whose mutual repulsion is responsible for the non-planar structure of both **1** and **2** [17], lie downfield of the corresponding protons in **3**, **4** and **7**, due to deshielding by two aromatic rings. The *Raman* spectra of **1** and **2** [18] are very similar, except in the region of 1600–1500 cm⁻¹; there are four very strong absorptions at 1595, 1578, 1572 and 1554 cm⁻¹ in **1**, but only one (at 1550 cm⁻¹) in **2**. The IR spectrum of **1** in the same region contains one weak absorption at 1552 cm⁻¹. The simplicity of the electronic spectrum of **1** in the UV/VIS region stands rather in contrast to those of **3** and **4** which contain isolated diazafluorenyl moieties (*Table 2*). The orange colour of **1** is recognised by the absorption at 416 nm (log ε 4.305), which is

assigned to a twisted intramolecular charge-transfer (TICT) transition [19]. This is at a significantly higher energy than the corresponding absorption [20] in **2** (λ_{\max} 455 nm, $\log \epsilon$ 4.344). The cyclic voltammetry of **1** in DMF solution indicates two quasi-reversible reductions at -0.67 V and -1.13 V (vs. SCE). These observations can be compared with those reported in [21] for **2** ($E_{1/2} = -1.10$ V (reversible), -1.50 V (quasi-reversible) vs. SCE in propylene carbonate/toluene 1 : 4) and show that the heterocycle is easier to reduce than the hydrocarbon. Reduction of **1** with 2% Na/Hg provides a green solution of the radical anion. The ESR spectrum of the anion comprises a single line ($g = 2.0021$ G), indicating that the electron is *localised* on the central olefinic bond. A semi-empirical molecular-orbital calculation (AM 1) of **1** confirms that the HOMO is mainly (C=C) π in character. These results can be compared with those reported in [22] for the reduction of **2**; in this case, the ESR spectrum shows much fine structure from which it is deduced that the unpaired electron is *delocalised* throughout the molecule.

Table 1. NMR Chemical Shifts (δ /ppm) and Coupling Constants (J/Hz). All spectra were recorded on solutions of the compounds in CDCl_3

¹ H-NMR										
Compound	H-C(3), H-C(6)			H-C(2), H-C(7)			H-C(1), H-C(8)			Other H-atoms
	δ	³ J	⁴ J	δ	³ J	⁴ J	δ	³ J	⁴ J	
1	8.77	4.8	1.4	7.31	4.8	8.0	8.43	8.0	1.4	
2^a	7.29	7.6	1.2	7.41	1.0	7.4	8.46	7.1		7.85
3	8.73	4.9	1.6	7.29	4.8	7.6	7.87	7.6	1.7	3.86
4	8.63	4.9	1.4	7.09	5.0	7.7	7.26	7.7	1.6	4.81
7	8.81	5.2	1.6	7.37	5.1	7.5	8.00	7.7	1.6	

¹³ C-NMR						
Compound	C(3), C(6)	C(2), C(7)	C(1), C(8)	C(4a), C(4b)	C(8a), C(9a)	C(9)
1	151.41	122.91	133.52	158.48	131.89	136.52
13	149.41	122.52	132.76	158.87	137.32	32.19
4	150.55	122.87	138.09	158.71	131.72	44.70
7	155.24	124.75	131.49	163.44	129.37	189.54

^a) From [17].

Table 2. Electronic Absorption Spectra in CHCl_3 Solution

Compound	λ_{\max}/nm ($\log \epsilon$)
1	244 (4.31) 311 (4.12) 416 (4.31)
2^a	244 (4.89), 272 (4.60), 281 (4.54) 455 (4.34)
3	244 (3.53) 297 (4.26), 304 (4.29), 310 (4.39)
4	229 (4.83), 260 (4.27) 300 (4.83), 307 (4.63), 313 (4.76)
7	244 (3.53) 303 (3.81), 310 (3.75), 317 (3.85), 340 (3.08)

^a) From [20].

Conclusive evidence for the identity of the orange solid **1** was obtained from the determination of the molecular structure by X-ray diffraction (*Fig. 1*). The bond lengths and inter-bond angles are given in *Table 3*. *Fig. 1, b*, shows that the two diazafluorenylidene fragments are each nearly planar (maximum deviation 0.1 Å), and

the dihedral angle between these planes is 37.8° . The corresponding angle in the β -form of hydrocarbon **2** [10] is 39.3° . The inter-ring double bond $C(1A)=C(1B)$ ($1.385(4)$ Å) is comparable to that in **2** ($1.364(15)$ Å). The mutual interference between the non-bonded H-atoms $C(3A)-H \cdots H-C(12B)$ and $C(12A)-H \cdots H-C(3B)$, which are at distances of $2.204(5)$ Å and $2.233(5)$ Å apart, respectively, is responsible for the observed distortion of the olefinic linkage. The molecular conformation is chiral, and both mirror-related conformations are present in the centrosymmetric crystal structure. This is an interesting class of compound, twisted [23] into a chiral conformation by

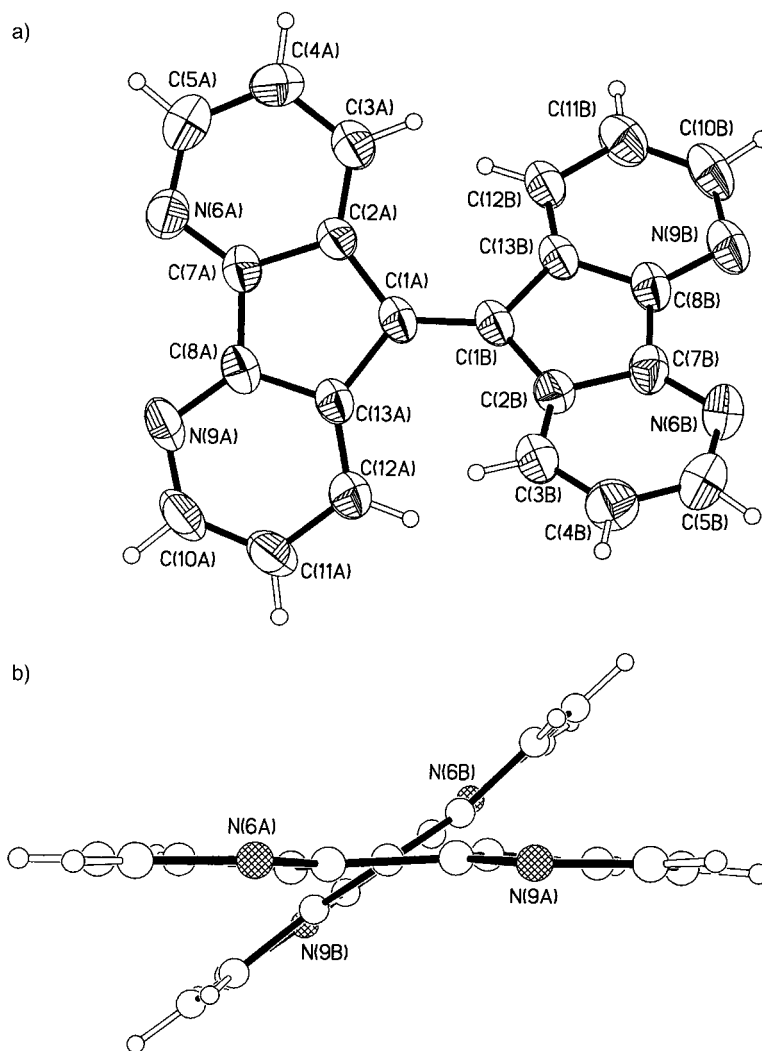


Fig. 1. Two views of the molecular structure of **1**: a) perpendicular to one half of the molecule (with anisotropic displacement parameters drawn at the 50% level), b) along the $C(1A)=C(1B)$ bond, showing the non-planar conformation

steric effects, and related to materials such as **8** [24]. Compound **1**, which does not racemise under normal conditions by rotation about the central bond, since this would involve breaking a π bond, has potential for use in the construction of chiral supramolecular systems. The averaged geometry of the four pyridine rings of **1** shows that the main effect of fusion to the five-membered ring is that the fused bond (1.412 Å) is lengthened by 0.03 Å compared to the unfused equivalent bond. The average length of the bond linking the pyridine ring to the bridgehead alkene is 1.478(5) Å, and the mean endocyclic angle at the bridgehead is 106.0(3)°.

We have also determined the structures of 4,5-diaza-9*H*-fluorene (**3**, Fig. 2), and 9,9'-bi-4,5-diaza-9*H*-fluorenyl (**4**; Fig. 3) in the crystalline state at room temperature, for the purposes of further comparison with their hydrocarbon analogues and with **1** (Table 3). Both pyridine rings of **3** are planar (maximum deviation 0.004(2) Å) and the dihedral angle between their best planes is 2.51(4)°; this may be compared with the room-temperature structure of fluorene [24], in which the dihedral angle is 0.8(2)°. Compound **4** adopts a *gauche* conformation about the bond linking the 4,5-diazofluorenyl moieties (Fig. 3). The torsion angle H–C–C–H about the aliphatic link is 67.39(6)°, and the length of this bond (1.542(3) Å) is the same as in 9,9'-bifluorenyl [25], for which a *gauche* conformation has also been established. Comparison of the averaged geometric structures for **3** and **4** with that of **1** shows that the effect of the bridgehead C=C bond is to decrease the length of the bonds between the bridgehead position and the pyridine rings from an average value of 1.512(2) Å in **3** and **4** to 1.478(5) Å in **1**, indicating some conjugation, and to lengthen the bond at the fusion of the pyridine rings to the five-membered ring from a mean value of 1.393(2) Å in **3** and **4** to 1.412(4) Å in **1**. The corresponding unfused bond in the

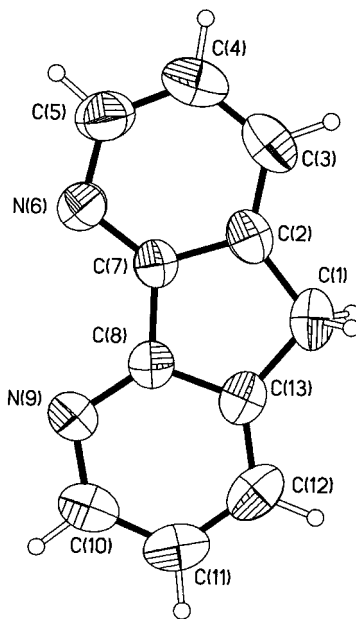


Fig. 2. The molecular structure of **3** (with anisotropic displacement parameters drawn at the 50% level)

pyridine ring in **3** and **4** is also slightly lengthened in **1**. The endocyclic angle at the bridgehead is increased from an average of $102.2(1)^\circ$ (in **3** and **4**) to $106.0(3)^\circ$ (in **1**). The effect of the bridging C-atom, C(1), in **1**, **3** and **4** in distorting the bipyridine portions of these molecules is most easily recognised when the average interbond angles in the fragment, N(6)–C(7)–C(8)–N(9) (**1**, 126.2° ; **3**, 126.3° ; **4**, 126.0°) are compared with the corresponding angle in 2,2'-bipyridine [26] (116.1°). The effect of the greater bite-angle in **3** on the coordination chemistry of Pd⁰ and Pt-*p*-quinone complexes was reported recently [27]. When the comparable angles in **2** [10] (130.2°), fluorene [28] (131.0°) and 9,9'-bifluorenyl [26] (130.5°) are matched with those in biphenyl and related molecules (121.1°), a similar distortion is noted.

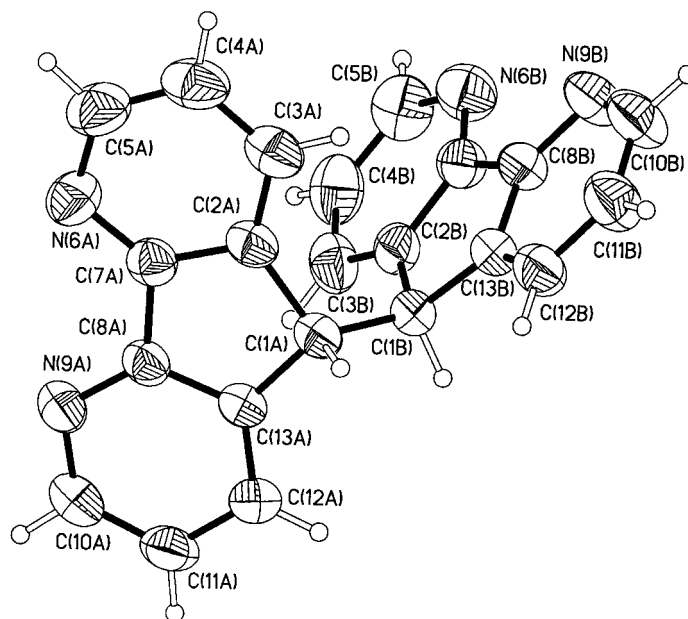


Fig. 3. A view of the molecular structure of **4** showing the gauche conformation about the central single bond (anisotropic displacement parameters drawn at the 50% probability level)

Thermolysis of **1** (750 K, sealed glass tube, 2.5 h) gave only **3**, in addition to decomposition products. The pK_a values of protonated **1**, **3** and **7**, taken with the corresponding value [29] for 4,5-diazaphenanthrene, show that **1** is the most basic of these molecules in solution (Table 4).

Following the known behaviour of the hydrocarbon **2**, which forms a donor-acceptor complex with 7,7,8,8-tetracyanoquinodimethane (TCNQ), the structure of which has been determined [30], we have prepared the corresponding complex of **1**. The bright red crystals of BDAF·TCNQ (**9**) are soluble in Me₂SO. The ¹H-NMR spectrum of **9** shows significant deshielding of both H–C(1)/H–C(8) and H–C(2)/H–C(7) compared to free **1**. The UV/VIS spectrum of **9** in MeCN solution shows two weak absorptions at 743 and 842 nm, which may be attributed [31] to charge-transfer

Table 3. Bond Lengths and Angles for Compounds **1**, **3** and **4**, and the Heterocyclic Component of Complex **9**

Bond lengths/Å	1		3	4		Complex 9	
C(1A)–C(1B)	1.386(4)			1.544(2)		1.371(4)	
	Side A	Side B		Side A	Side B	Side A	Side B
C(1)–C(2)	1.470(5)	1.470(5)	1.499(2)	1.517(2)	1.513(2)	1.483(3)	1.483(3)
C(1)–C(13)	1.489(5)	1.485(4)	1.504(2)	1.511(2)	1.510(2)	1.483(3)	1.473(3)
C(2)–C(3)	1.377(5)	1.380(5)	1.378(2)	1.381(2)	1.380(2)	1.379(3)	1.385(3)
C(2)–C(7)	1.420(4)	1.414(4)	1.394(2)	1.396(2)	1.399(2)	1.404(3)	1.405(3)
C(3)–C(4)	1.391(5)	1.377(5)	1.380(2)	1.380(3)	1.385(3)	1.384(3)	1.381(3)
C(4)–C(5)	1.390(5)	1.404(5)	1.372(2)	1.377(3)	1.377(3)	1.375(3)	1.387(3)
C(5)–N(6)	1.341(5)	1.334(5)	1.336(2)	1.341(2)	1.334(2)	1.339(3)	1.341(3)
C(7)–N(6)	1.331(4)	1.331(4)	1.337(2)	1.336(2)	1.341(2)	1.339(3)	1.340(3)
C(7)–C(8)	1.457(5)	1.464(5)	1.467(2)	1.470(2)	1.467(2)	1.462(3)	1.462(3)
C(8)–N(9)	1.337(4)	1.347(4)	1.336(2)	1.338(2)	1.339(2)	1.337(3)	1.336(3)
C(8)–C(13)	1.411(5)	1.403(4)	1.395(2)	1.390(2)	1.394(2)	1.409(3)	1.410(3)
C(10)–N(9)	1.334(5)	1.343(5)	1.340(2)	1.336(2)	1.335(2)	1.333(3)	1.340(3)
C(10)–C(11)	1.388(5)	1.370(5)	1.374(2)	1.376(2)	1.381(3)	1.381(3)	1.380(3)
C(11)–C(12)	1.392(4)	1.384(5)	1.374(2)	1.382(2)	1.382(2)	1.381(3)	1.381(3)
C(12)–C(13)	1.377(5)	1.379(5)	1.379(2)	1.381(2)	1.373(2)	1.378(3)	1.384(3)
<i>Angles/°</i>	1		3	4		Complex 9	
C(2A)–C(1A)–C(1B)	128.7(3)			116.09(12)		127.4(2)	
C(13A)–C(1A)–C(1B)	125.4(3)			113.74(13)		127.1(2)	
C(1A)–C(1B)–C(2B)	127.0(3)			116.51(12)		126.9(2)	
C(1A)–C(1B)–C(13B)	126.9(3)			113.96(12)		127.6(2)	
	Side A	Side B		Side A	Side B	Side A	Side B
C(2)–C(1)–C(13)	105.9(3)	106.0(3)	102.8(1)	101.85(12)	102.10(12)	105.5(2)	105.5(2)
C(1)–C(2)–C(3)	133.0(3)	133.0(3)	131.5(1)	131.71(14)	131.15(14)	132.8(2)	133.1(2)
C(1)–C(2)–C(7)	108.5(3)	108.6(3)	110.3(1)	110.33(12)	110.27(14)	108.7(2)	108.8(2)
C(3)–C(2)–C(7)	117.6(3)	117.4(3)	118.2(1)	117.94(15)	118.5(2)	117.6(2)	117.6(2)
C(2)–C(3)–C(4)	118.2(4)	118.5(4)	117.5(1)	117.4(2)	117.4(2)	117.5(2)	117.8(2)
C(3)–C(4)–C(5)	119.1(4)	119.2(4)	119.9(1)	120.2(2)	119.5(2)	120.1(2)	119.8(2)
C(4)–C(5)–N(6)	124.5(4)	124.0(4)	124.6(2)	124.2(2)	125.0(2)	124.4(2)	124.4(2)
C(2)–C(7)–C(8)	108.6(3)	108.3(3)	108.4(1)	108.52(13)	108.51(14)	108.8(2)	108.5(2)
C(2)–C(7)–N(6)	125.2(3)	125.4(4)	125.2(1)	125.69(14)	124.9(2)	125.5(2)	125.6(2)
C(8)–C(7)–N(6)	126.1(3)	126.1(3)	126.3(1)	125.78(14)	126.61(15)	125.7(2)	125.9(2)
C(7)–C(8)–C(13)	108.6(3)	108.8(3)	108.4(1)	108.36(13)	108.41(13)	108.5(2)	108.4(2)
C(7)–C(8)–N(9)	126.5(3)	125.5(3)	126.4(1)	126.22(13)	126.93(14)	126.2(2)	126.0(2)
C(13)–C(8)–N(9)	124.7(4)	125.7(3)	125.3(1)	125.42(13)	124.7(2)	125.2(2)	125.6(2)
C(11)–C(10)–N(9)	125.1(3)	125.2(4)	124.9(2)	124.40(15)	125.1(2)	124.5(2)	124.5(2)
C(10)–C(11)–C(12)	119.0(4)	119.9(4)	119.6(4)	120.03(15)	119.2(2)	119.9(2)	119.6(2)
C(11)–C(12)–C(13)	117.5(3)	117.5(4)	117.8(1)	117.14(15)	117.4(2)	117.6(3)	118.2(2)
C(1)–C(13)–C(12)	132.3(3)	133.3(3)	131.7(1)	130.70(14)	130.23(14)	133.0(2)	133.2(2)
C(1)–C(13)–C(18)	108.3(3)	108.3(3)	110.2(1)	110.90(12)	110.68(14)	108.5(2)	108.9(2)
C(8)–C(13)–C(12)	118.6(3)	117.9(3)	118.2(1)	118.39(14)	119.09(14)	117.7(2)	117.1(2)
C(5)–N(6)–C(7)	115.1(3)	115.3(3)	114.7(1)	114.54(15)	114.7(2)	114.6(2)	114.5(2)
C(8)–N(9)–C(10)	114.8(3)	113.6(3)	114.3(1)	114.60(13)	114.55(15)	114.7(2)	114.7(2)

transitions from BDAF to TCNQ, in addition to absorptions at 311 and 394 nm, characteristic of the components. The *Raman* spectrum of solid **9** shows an absorption at 2224 cm⁻¹ which is very little changed from the value of $\nu(\text{CN})$ in TCNQ, suggesting that little charge is transferred to the acceptor. The absorptions at 1553 and 1570 cm⁻¹ are unchanged, and the absorptions at 1578 and 1594 cm⁻¹ in **1** are shifted only slightly

Table 4. pK_a Values of the Conjugated Acids of Selected Diaza-heterocyclic Systems

9,9'-Bi-4,5-diaza-9 <i>H</i> -fluorenylidene (1)	5.90 ± 0.06
4,5-Diaza-9 <i>H</i> -fluorene (3)	4.21 ± 0.03
4,5-Diaza-9 <i>H</i> -fluoren-9-one (7)	5.77 ± 0.05
1,10-Diazaphenanthrene	4.95 ± 0.03

to higher wavenumbers (1586 and 1596 cm^{-1}) in **9**, however the *intensities* of these absorptions decrease by 10 and 50%, respectively.

The structure of the BDAF·TCNQ (**9**) was determined by a single-crystal X-ray diffraction study, and the asymmetric unit is shown in Fig. 4. Bond lengths and interbond angles for the BDAF component are listed in Table 3, for ease of comparison with those of uncomplexed **1**, and selected parameters for the TCNQ component are in Table 5. On complexation, the dihedral angle between the diazafluorenylidene planes in the BDAF molecule has decreased only slightly from 37.8° in **1** to 35.3° in **9**. In the solid state, the complex takes the form of an infinite spiral stack parallel to the *b*-axis of the crystal which is illustrated in Fig. 5. The spine of the stack is composed of the **A**

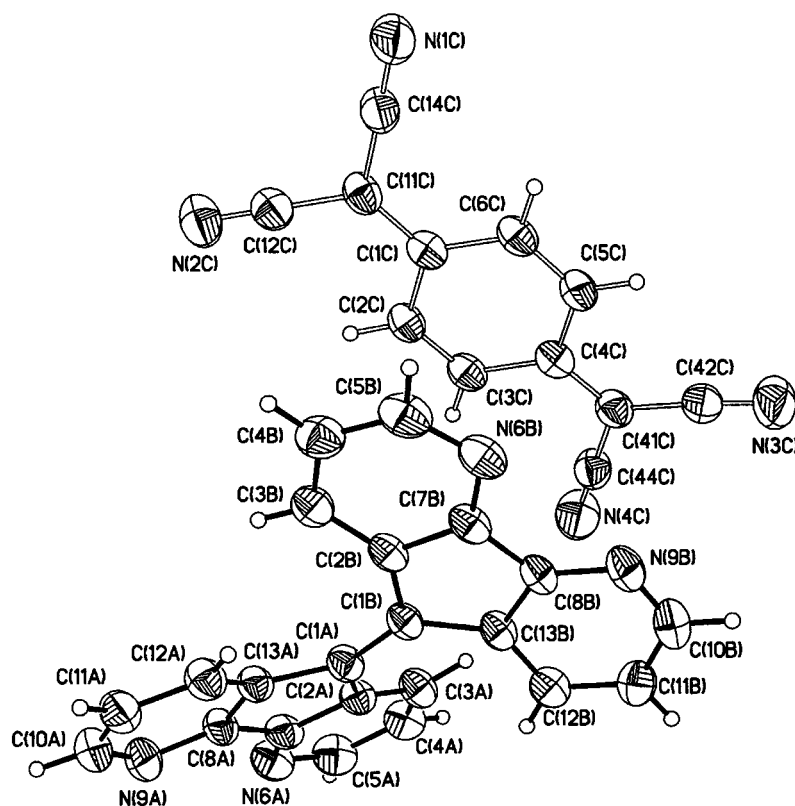


Fig. 4. The asymmetric unit in the crystal of the donor/acceptor complex BDAF·TCNQ (**9**) (anisotropic displacement parameters drawn at the 50% probability level)

halves of the BDAF molecules each held by π - π interactions between the two pyridyl groups and the adjacent BDAF units (*Fig. 6,a*). Neighbours are related by a twofold screw axis. As a consequence of this arrangement, the **B** halves of the BDAF molecules project out forming two arrays along the outside of the stack. The **B** units along one side of the stack are related by successive unit-cell translations in the *b*-direction, and are, therefore, exactly parallel to each other, each being tilted at an angle of 35.3° to the corresponding central **A** units; the **B** units on the opposite side are similarly arranged but tilted in the opposite direction being related to those on the first side by the 2_1 -axis (*Fig. 5*). The TCNQ molecules slot into the gaps between adjacent **B** units on both sides of the stack and are held by π - π interactions involving the central phenylene ring and two CN groups. The oblique orientation of the **B** units of the BDAF molecule

Table 5. Selected Bond Lengths and Angles of the TCNQ Component of the Complex **9** (those for the BDAF component are listed in Table 3)

Bond lengths / Å			
C(1C)–C(6C)	1.444(3)	C(1C)–C(11)	1.369(3)
C(2C)–C(3C)	1.340(3)	C(3C)–C(4C)	1.441(3)
C(4C)–C(41C)	1.368(3)	C(4C)–C(5C)	1.442(3)
C(5C)–C(6C)	1.339(3)	C(11C)–C(12C)	1.433(3)
C(11C)–C(14C)	1.427(3)	C(12C)–N(2C)	1.143(3)
C(14C)–N(1C)	1.143(3)	C(41C)–C(44C)	1.434(3)
C(41C)–C(42C)	1.430(3)	C(42C)–N(3C)	1.142(3)
C(44C)–N(4C)	1.138(3)	C(1C)–C(2C)	1.449(3)
Bond angles / °			
C(1C)–C(11C)–C(12C)	122.2(2)	C(1C)–C(11C)–C(14C)	122.7(2)
C(12C)–C(11C)–C(14C)	115.0(2)	N(2C)–C(12C)–C(11C)	179.3(2)
N(1C)–C(14C)–C(11C)	177.4(3)	C(4C)–C(41C)–C(44C)	122.3(2)
C(4C)–C(41C)–C(42C)	123.9(2)	C(44C)–C(41C)–C(42C)	113.8(2)
N(3C)–C(42C)–C(41C)	176.7(3)	N(4C)–C(44C)–C(41C)	178.7(3)

results in a CN group at one end of the TCNQ molecule interacting with a BDAF **B** below it and a second CN group at the other end interacting in an almost identical manner with the one above it (*Fig. 6,b*); in contrast, the central phenylene ring of the TCNQ molecule is partially ‘sandwiched’ between different pyridyl rings of symmetry-related BDAF **B** units. Between stacks there are also H-bonding interactions between outward pointing pairs of cyano N-atoms and the H-atoms H–C(3) and H–C(6) of the outer **B** side of a BDAF molecule in the next stack. Thus, a TCNQ and a BDAF molecule lie side by side such that there are a pair of N \cdots H–C contacts (2.44 and 2.46 Å, angles at H 156 and 159°, angles at N 122 and 123°, C–H bond lengths constrained to 0.93 Å in the refinement). The disposition of TCNQ molecules with respect to BDAF molecules is consistent with TICT in **1**, leading to a polar excited state [19][21][32] so that the acceptor TCNQ interacts preferentially with one region of the donor BDAF, the **B** half. The central olefinic bond of the BDAF component of **9** is slightly shorter (1.371(4) Å) than in **1** (1.386(4) Å), which is, in turn, consistent with a reduction in TICT. Otherwise the bond lengths and inter-bond angles in the complex are unchanged from their values in the free molecules. From the empirical correlation [33] between charge transferred to TCNQ and the bond lengths in that molecule, we

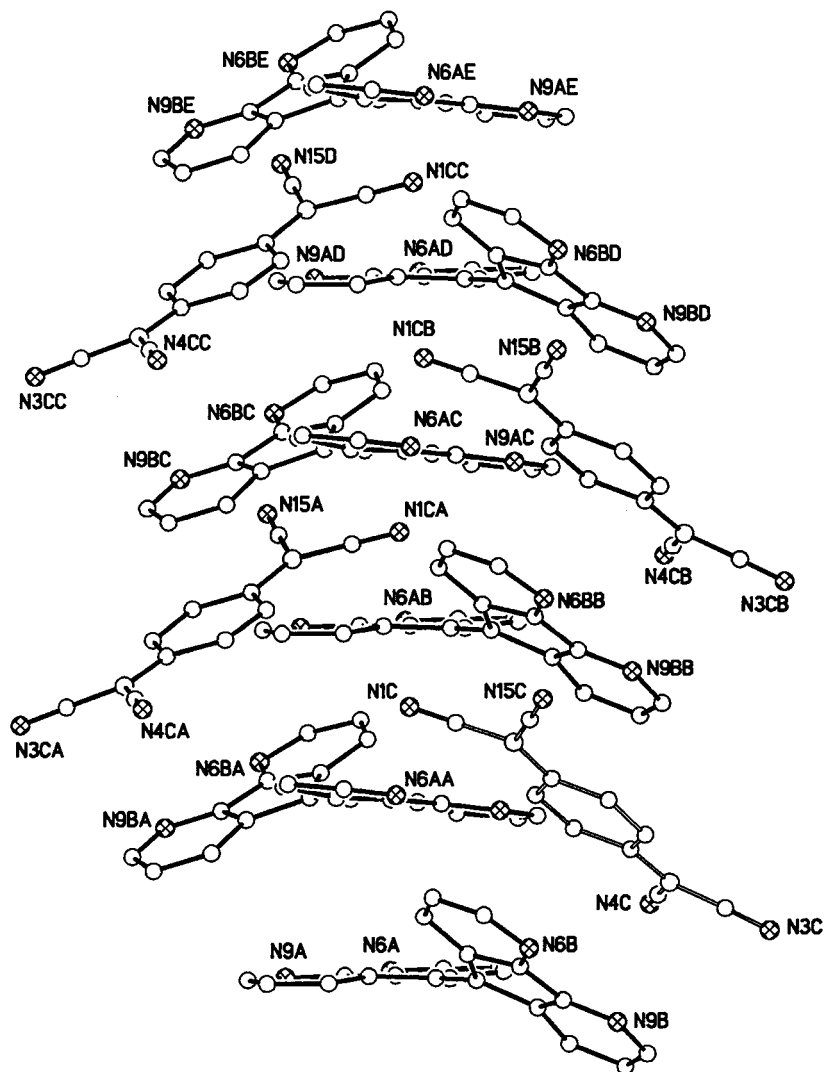


Fig. 5. The infinite spiral, triply π -stacked structure of **9** generated by the 2_1 axis of the crystal. The fourth symbol in the atomic designation denotes the following equivalent positions: A: $-x, 0.5 + y, 0.5 - z$; B: $x, 1 + y, z$; C: $-x, 1.5 + y, 0.5 - z$; D: $x, 2 + y, z$; E: $-x, 2.5 + y, 0.5 - z$.

conclude that the charge transfer from **1** is very small (0.05 electron), as was indicated by the infrared spectrum of **9**. Comparison with the structure [30] of the complex formed between TCNQ and **2**, the hydrocarbon analogue of **1**, is instructive in that the dihedral angle for **2** in the complex is almost the same as in free **2** (40° vs. 39°) and the olefinic bond length ($1.372(4)$ Å) in the complex is not significantly different from that in free **2** ($1.364(15)$ Å).

We have prepared coordination complexes of **1** with various 3d transition-metal dichlorides, MCl_2 , of the general compositions $[MCl_2L]$ ($M = Ni, Zn$) and $[(MCl_2)_2L]$

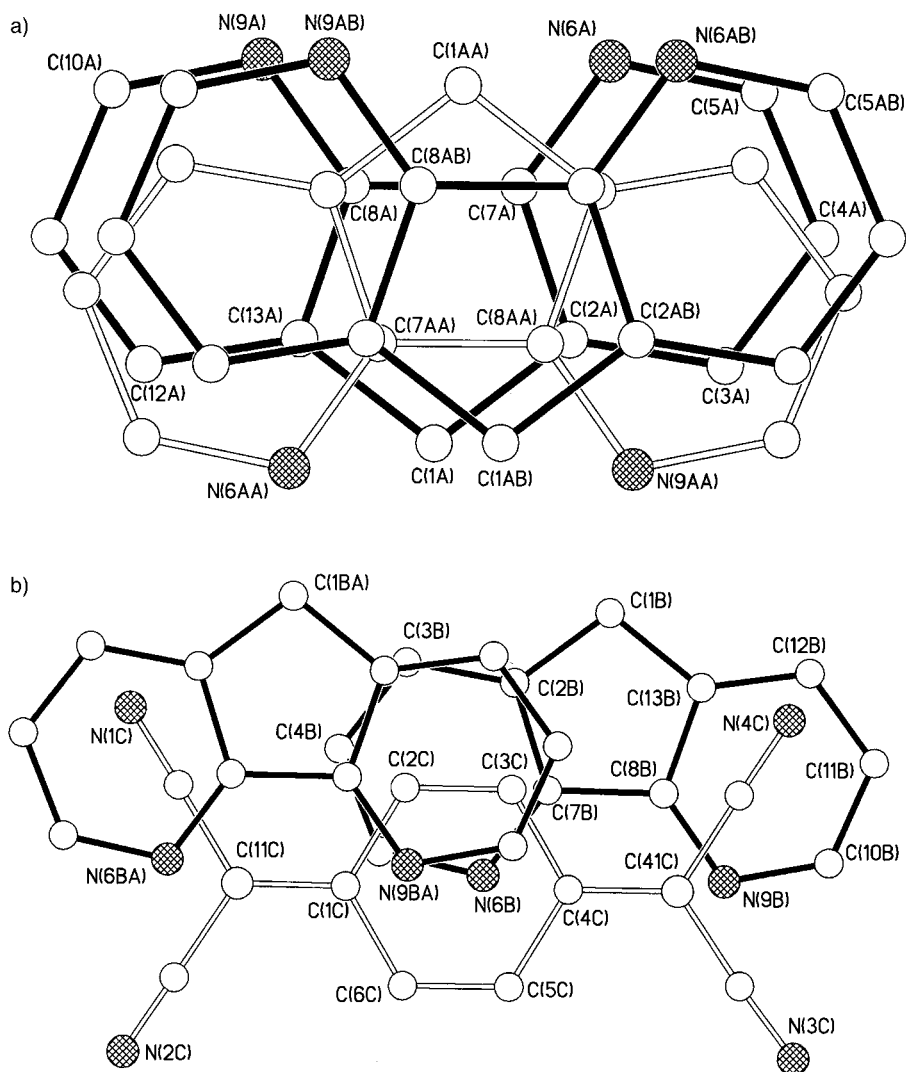


Fig. 6. Details of the π - π interactions in the infinite structure of **9**. The fourth symbol in the atomic label denotes the equivalent position A: $-x, 0.5 + y, 0.5 - z$; B: $x, 1 + y, z$. a) Three layers of the central stacking arrangement of the **A** halves of the BDAF molecules (viewed down the b -axis). The pyridyl group [N(9AA)] of the central molecule (open bonds) interacts with the second pyridyl [N(6A)] of the **A** unit *below* it, and the second central pyridyl group [N(6AA)] with the first [N(9AB)] of the **A** unit *above*. The dihedral angle between each pair of interacting pyridyl groups is 11.7° , with a mean separation of *ca.* 3.6 Å, and the rings are offset by 0.91 Å [35]. b) The π - π interactions between a TCNQ molecule and the **B** halves of two adjacent BDAF molecules. The central phenylene ring of the TCNQ molecule (open bonds) interacts both with the pyridyl ring [N(6B)] of the BDAF molecule *below* it and with the opposite pyridyl ring [N(9BA)] of that *above* it; the dihedral angle between adjacent rings is 0.5° and the rings are separated by 3.3 Å with a mean offset of 1.54 Å [35].

(M = Co, Ni, Zn) by standard methods. These complexes have been characterised by microanalysis and spectroscopy. The UV/VIS spectra of the complexes are dominated by the absorption due to BDAF at 416 nm, so the d–d transitions cannot be observed. The $^1\text{H-NMR}$ spectra of the two diamagnetic Zn^{II} complexes show the expected shift of the ring protons to lower field on coordination. We have also prepared [6] the Ru^{II} complexes, $[\text{Ru}(\text{bdaf})(\text{bpy})_2](\text{PF}_6)_2$ and $[\{\text{Ru}(\text{bpy})_2\}_2(\text{bdaf})]\text{X}_4$ ($\text{X} = \text{BF}_4, \text{PF}_6$) from $[\text{Ru}(\text{bpy})_2\text{Cl}_2]$ in the usual way. Detailed assignment of the NMR spectra of these Ru^{II} complexes has not been achieved. In mononuclear $[\text{Ru}(\text{bpy})_2(\text{bdaf})](\text{PF}_6)_2$, the signals of the protons of the uncoordinated fragment of BDAF are abnormally broad. This line broadening is solvent dependent, and disappears in the binuclear complexes. The use of COSY spectra enabled an assignment to be made of the proton NMR signals of the BDAF in these complexes. It is noteworthy that the coordination shift of H–C(3)/H–C(6) of the BDAF ligand, that is, of the protons adjacent to the donor N-atom in $[\text{Ru}(\text{bpy})_2(\text{bdaf})]^{2+}$ (– 1.14 ppm) and in $[\{\text{Ru}(\text{bpy})_2\}_2(\text{bdaf})]^{4+}$ (– 1.08 ppm) is much greater than in $[\{\text{ZnCl}_2\}_2(\text{bdaf})]$ (0.18 ppm). The luminescence of these two cationic Ru^{II} complexes is very weak and short-lived even at 77 K, when compared [34] with $[\text{Ru}(\text{bpy})_2(\mathbf{3})]^{2+}$ and with $[\text{Ru}(\text{bpy})_2(\mathbf{7})]^{2+}$. The redox behaviour of the complexes indicates that there is only weak interaction between the ruthenium ions in the binuclear complexes.

We have described the preparation and characterisation of an interesting chiral bis-bidentate proligand with two metal binding sites which has the potential for incorporation into supramolecular assemblies.

Experimental Part

General. Solvents and materials were used as received, unless otherwise stated. 1,10-Phenanthroline and *N*-bromosuccinimide were purchased from *Avocado*. Hydrazine hydrate, TCNQ, DDQ and DPPH were purchased from *Aldrich*. Compounds **3** and **4** were prepared according to the published [11][12] methods.

Uncorrected m.p. were measured on a *Shandon* hot-stage apparatus fitted with a microscope and type-7905 temp. regulator. IR Spectra of compounds prepared as *Nujol*TM mulls were recorded on a *Mattson Instruments Alpha Centauri* FT-IR spectrometer interfaced with an *AT&T UNIX* PC. $^1\text{H-}$ and $^{13}\text{C-NMR}$ spectra were measured on CDCl_3 solns. at r.t. (unless otherwise indicated) using a *JEOL GX270 FT* spectrometer by Dr. *D. O. Smith*. FAB Mass spectra were recorded at the EPSRC mass spectrometry service centre at the University of Wales, Swansea. *Raman* spectra were recorded using a *Coderg* model *PHO* spectrometer with a Kr ion laser (output 647.1 nm). ESR Spectra were recorded on a *JEOL PE-IX* instrument at r.t., at X-band (ca. 9 GHz); the frequency was measured with an attenuator device to ± 0.0005 GHz. A quartz tube (3 mm i.d.) was used; the *g* value was calibrated with DPPH ($g = 2.0036$ G).

X-Ray Crystal-Structure Determination of 1, 3, 4 and 9. The data were collected using a *Siemens P4* diffractometer; no significant decay in intensity of three standard reflections measured after every 100 reflections was observed. The data were corrected for *Lorentz* and polarisation factors but not for absorption; the details of the data collection and refinement for the four compounds are given in *Table 6*.

Structure Solution and Refinement. The four structures were all solved by direct methods and, in each case, all non-H-atoms were located from subsequent difference *Fourier* syntheses. All non-H-atoms were assigned anisotropic displacement parameters and refined using full-matrix least squares [35] on F_o^2 . The H-atoms were included at calculated positions with C–H bond distances of 0.93 and 0.98 Å for the aromatic and aliphatic H-atoms, respectively. During refinement, all H-atoms were allowed to ride on their parent atom and were assigned isotropic thermal parameters equal to $1.2 U_{\text{eq}}$ Å² of the parent atom. Complete atomic coordinates, thermal parameters and bond lengths and angles have been deposited at the *Cambridge Crystallographic Data Centre*. The data have been given the following deposition numbers: **1**, CCDC 110269; **3**, CCDC 110270; **4**, CCDC 110271; **9** CCDC 110272.

Table 6. Details of Data Collection and Refinement for Compounds **1**, **3**, **4** and **9**

Compound	1	3	4	9
Empirical formula	C ₂₂ H ₁₂ N ₄	C ₁₁ H ₈ N ₂	C ₂₂ H ₁₄ N ₄	C ₃₂ H ₁₆ N ₈
Temp. [K]	293 (2)	296 (2)	296 (2)	296 (2)
Wavelength [Å]	0.71073	0.71073	0.71073	0.71073
Crystal system	Monoclinic	Monoclinic	Monoclinic	Monoclinic
Space group	<i>P</i> 2 ₁ / <i>c</i>	<i>P</i> 2 ₁ / <i>n</i>	<i>P</i> 2 ₁ / <i>c</i>	<i>P</i> 2 ₁ / <i>c</i>
Unit cell dimensions				
<i>a</i> [Å]	12.302 (2)	6.2088 (4)	12.7934 (9)	11.4667 (6)
<i>b</i> [Å]	11.503 (2)	11.4488 (11)	11.6538 (9)	7.7356 (2)
<i>c</i> [Å]	12.079 (2)	12.1047 (8)	11.0140 (13)	28.5667 (14)
β [°]	110.61 (2)	98.101 (6)	93.984 (8)	95.243 (5)
Volume [Å ³], <i>Z</i>	1602.3 (5), 4	851.86 (11), 4	1638.1 (3), 4	2523.3 (2), 4
Density (calculated) [Mg/m ³]	1.378	1.311	1.356	1.412
Absorption coefficient [mm ⁻¹]	0.085	0.080	0.083	0.706
<i>F</i> (000)	688	352	696	1104
Crystal size [mm]	0.57 × 0.48 × 0.19	0.44 × 0.40 × 0.36	0.48 × 0.44 × 0.44	0.42 × 0.36 × 0.18
θ Range for data collection	1.77 to 25.00°	2.46 to 24.99°	1.60 to 25.00°	3.11 to 55.00°
Limiting indices	–14 ≤ <i>h</i> ≤ 14 –13 ≤ <i>k</i> ≤ 13 –14 ≤ <i>l</i> ≤ 14	–7 ≤ <i>h</i> ≤ 7 –13 ≤ <i>k</i> ≤ 13 –14 ≤ <i>l</i> ≤ 14	–15 ≤ <i>h</i> ≤ 15 –13 ≤ <i>k</i> ≤ 13 –13 ≤ <i>l</i> ≤ 13	–1 ≤ <i>h</i> ≤ 12 –1 ≤ <i>k</i> ≤ 8 –30 ≤ <i>l</i> ≤ 30
Reflections collected	5918	3280	11204	4423
Independent reflections	2824		1504	2883
<i>R</i> _{int}	0.0765	0.0176	0.0259	0.0185
Data/restraints/parameters	2824/ 0 /235	1504/ 0 /119	2882/ 0 /235	3179/ 0 /379
Goodness of fit on <i>F</i> ²	1.005	1.031	1.007	1.046
Final <i>R</i> 1, <i>wR</i> 2 [<i>I</i> > 2σ(<i>I</i>)]	0.0637, 0.1224	0.0354, 0.0916	0.0390, 0.0975	0.0433, 0.1003
Final <i>R</i> 1, <i>wR</i> 2 (all data)	0.1477, 0.1562	0.0463, 0.0990	0.0540, 0.1109	0.0589, 0.1097
Max. diffraction peak/hole [e Å ⁻³]	0.194, –0.245	0.153, –0.133	0.118, –0.156	0.138, –0.215

9-Bromo-4,5-diaza-9H-fluorene (5). Solid *N*-bromosuccinimide (NBS; 1.10 g, 6.18 mmol) was added to a soln. of 4,5-diaza-9H-fluorene (**3**, 1.0 g, 5.95 mmol) in dry (CaH₂) benzene (50 ml). The mixture was heated to reflux under N₂ overnight. The cooled mixture was filtered to remove succinimide, and the solvent was then removed by distillation under reduced pressure to give a yellow residue which is a mixture of mono- and dibromo-4,5-diaza-9H-fluorene. These two compounds were separated by column chromatography (silica gel; CHCl₃/MeCN 7:3). Compound **5** was recrystallised from toluene as off-white crystals (0.89 g, 61%). M.p. 121–122°. UV: λ_{max} (log ε) 318 (4.110), 304 (4.041), 246 (4.064). ¹H-NMR: 8.74 (*dd*, *J* = 4.7, 1.1, H–C(3), H–C(6)); 7.98 (*dd*, *J* = 1.4, 7.7, H–C(1), H–C(8)); 7.36 (*dd*, *J* = 4.9, 7.7, H–C(2), H–C(7)); 5.97 (*s*, H–C(9)). ¹³C-NMR: 157.33 (C(4a), C(4b)); 151.27 (C(3), C(6)); 139.15 (C(8a), C(9a)); 133.85 (C(1), C(8)); 123.73 (C(2), C(7)); 39.99 (C(9)). MS: 247 (8, *M*⁺), 167 (100). Anal. calc. for C₁₁H₇BrN₂: C 53.5, H 2.9, N 11.3; found: C 53.8, H 3.0, N 11.3.

9,9'-Dibromo-9,9'-bi-4,5-diaza-9H-fluorenyl (6) was purified by recrystallisation from ethanol as white crystals (0.32 g, 16%). M.p. 227–229°. λ_{max} (log ε): 320 (4.120), 310 (4.04), 244 (4.064). ¹H-NMR: 8.73 (*dd*, *J* = 4.8, 1.1, H–C(3), H–C(6)); 8.16 (*dd*, *J* = 7.5, 1.5, H–C(1), H–C(8)); 7.44 (*dd*, *J* = 8.0, 5.0, H–C(2), H–C(7)). ¹³C-NMR: 153.22 (C(4a), C(4b)); 152.19 (C(3), C(6)); 143.95 (C(8a), C(9a)); 133.34 (C(1), C(8)); 124.86 (C(2), C(7)); 46.11 (C(9)). MS: 326 (9, *M*⁺), 245 (100). Anal. calc. for C₁₁H₆Br₂N₂: C 40.5, H 1.9, N 8.6; found: C 40.4, H 1.8, N 8.7.

9,9'-Bi-4,5-diaza-9H-fluorenylidene (1). *Method 1*: A sat. soln. of *t*-BuOK in *t*-BuOH (20 ml) was added to a soln. of **5** (0.35 g, 1.416 mmol) in *t*-BuOH (20 ml), and the mixture was then heated to reflux under N₂ (0.25 h). The mixture was allowed to cool to r.t., and then the black precipitate was removed by filtration before being dried under vacuum. The dry precipitate was dissolved in H₂O (50 ml) and extracted with CHCl₃ (4 × 50 ml). The combined extracts were dried (MgSO₄), filtered, and then the solvent was removed by distillation under

reduced pressure, leaving a dark solid. The solid was purified by chromatography (silica gel; $\text{CHCl}_3/\text{MeCN}$ 7:3) to give **1** as an orange powder (0.21 g, 89%).

Method 2: Solid NBS (0.57 g, 3.20 mmol) and a catalytic amount of dibenzoyl peroxide (0.05 g) were added to a soln. of **4** (1.0 g, 3.0 mmol) in CHCl_3 (60 ml). The mixture was heated at reflux (5 h), during which time the initially yellow soln. turned red and a reddish-orange precipitate formed. The cooled mixture was filtered, and the precipitate was partitioned between H_2O and CHCl_3 (1:1; 100 ml). The aq. layer was re-extracted with CHCl_3 (3×100 ml). The combined org. extracts were dried (MgSO_4), filtered and then concentrated to give an orange solid, which was purified by chromatography as described before to give **1** (0.85 g, 86%).

Method 3: The dehydrogenation of **4** by the action of DDQ has already been described in [6]. In addition to the data recorded there for **1**, the following are relevant: IR: 1552w, 1260w, 1170m, 1110w, 1030w, 810m. Raman: 1595vs, 1578vs, 1572vs, 1554vs, 1478w, 1353w, 1219s, 1211s, 1167m, 1110m, 1037s, 813m, 794w, 490s, 318s, 310s. MS: 332 (100, M^+), 167 (10), 97 (3), 84 (3).

Preparation of the Complex 9. Commercial TCNQ was recrystallised from MeCN before use. A soln. of TCNQ (0.046 g, 0.226 mmol) in THF (15 ml) was added dropwise over 0.5 h to a soln. of BDAF (0.075 g, 0.226 mmol) in CHCl_3 (6 ml). The mixture was stirred at r.t. for 2 h. Red crystals, which formed rapidly (30 s), were isolated by filtration, washed with CHCl_3 and Et_2O , and dried in vacuum (0.104 g, 86%). $^1\text{H-NMR}$ ((D_6) DMSO): 8.73 (t, $J = 5.2$, H-C(3), H-C(6)); 8.58 (d, $J = 7.7$, H-C(1), H-C(8)); 7.49 (dd, $J = 5.0$, 7.6, H-C(2), H-C(7)). Raman: 3075vw, 3067vw, 3026vw, 2224s, 1598s, 1586s, 1570vs, 1553vs, 1460vs, 1226s, 1210s, 1200s, 1030s. Anal. calc. for $\text{C}_{34}\text{H}_{16}\text{N}_8$: C 70.6, H 2.0, N 27.4; found: C 70.6, H 1.8, N 27.6.

$[(\text{CoCl}_2)_2(\text{bdaf})] \cdot 2 \text{H}_2\text{O}$. A soln. of anh. CoCl_2 (39 mg, 0.3 mmol) in dry EtOH (2 ml) was added to a soln. of BDAF (50 mg, 0.15 mmol) in CHCl_3 (4 ml). After stirring the mixture for 0.5 h, the green solid product was isolated by filtration, washed with CHCl_3 and EtOH, and dried in vacuum. Yield: 54 mg (62%). IR: 3374m (br.), 1626w, 1302s, 1168s, 1124m, 765w. FAB-MS: 520 (12, M^+), 426 (100). Anal. calc. for $\text{C}_{22}\text{H}_{16}\text{Cl}_4\text{Co}_2\text{N}_4\text{O}_2$: C 42.1, H 2.6, N 8.9, found: C 41.9, H 2.8, N 8.9.

$[\text{NiCl}_2(\text{bdaf})]$. A soln. of $\text{NiCl}_2 \cdot 6 \text{H}_2\text{O}$ (40 mg, 0.168 mmol) in EtOH (4 ml) was added to a soln. of BDAF (50 mg, 0.15 mmol) in CHCl_3 (6 ml), and the mixture was stirred for 1 h at r.t. A green precipitate was formed, which was isolated by filtration. The yellow filtrate was concentrated (3 ml), and more precipitate was obtained. The combined solid products were washed with CHCl_3 and ice-cold EtOH, then dried in vacuum to give a green solid. Yield: 56 mg, 81%. FAB-MS: 427 (27, M^+), 391 (100). Anal. calc. for $\text{C}_{22}\text{H}_{12}\text{Cl}_2\text{N}_4\text{Ni}$: C 57.2, H 2.6, N 12.1; found: C 56.9, H 2.8, N 11.9.

$[(\text{NiCl}_2)_2(\text{bdaf})]$. A soln. of $\text{NiCl}_2 \cdot 6 \text{H}_2\text{O}$ (161 mg, 0.68 mmol) in EtOH (7 ml) was added to a soln. of BDAF (60 mg, 0.181 mmol) in CHCl_3 (8 ml), and the mixture was stirred for 1 h at ambient temp. The yellow-green precipitate was isolated by filtration, washed with CHCl_3 and EtOH, and then dried in vacuum. The product was recrystallised from EtOH as pale green crystals. Yield: 71 mg (71%). Anal. calc. for $\text{C}_{22}\text{H}_{12}\text{Cl}_4\text{N}_4\text{Ni}_2$: C 44.7, H 2.2, N 9.5; found: C 44.7, H 2.3, N 9.3.

$[\text{ZnCl}_2(\text{bdaf})]$. A soln. of ZnCl_2 (33 mg, 0.24 mmol) in EtOH (2 ml) was added to a soln. of BDAF (75 mg, 0.226 mmol) in CHCl_3 (10 ml), and the mixture was stirred for 0.5 h at ambient temp. The orange precipitate was isolated by filtration, washed with CHCl_3 and ice-cold H_2O , and dried in vacuum. The yellow powder was recrystallised from EtOH. Yield: 86 mg (81%). IR: 1570s, 1306w, 1168w, 888m, 810m, 740m. FAB-MS: 468 (3, M^+), 105 (100). Anal. calc. for $\text{C}_{22}\text{H}_{12}\text{Cl}_2\text{N}_4\text{Zn}$: C 56.4, H 2.6, N 11.9; found: C 56.2, H 2.8, N 11.6.

$[(\text{ZnCl}_2)_2(\text{bdaf})]$. A soln. of ZnCl_2 (85 mg, 0.624 mmol) in EtOH (2 ml) was added to a soln. of BDAF (90 mg, 0.27 mmol) in CHCl_3 (10 ml), and the mixture was stirred for 0.5 h at ambient temp. Filtration of the cooled mixture provided an orange precipitate which was washed with CHCl_3 and then dried in vacuum. The orange-yellow powder was recrystallised from EtOH. Yield: 126 mg, 77%. IR: 1560s, 1168s, 1123m, 890m, 740m, 456m. $^1\text{H-NMR}$ ((D_6) DMSO): 8.73 (dd, $J = 1.4$, 4.8, H-C(3), H-C(3'), H-C(6), H-C(6')); 8.57 (dd, $J = 1.4$, 8.0, H-C(1), H-C(1'), H-C(8), H-C(8')); 7.49 (dd, $J = 8.0$, 4.7, H-C(2), H-C(2'), H-C(7), H-C(7')). FABMS: 534 (12, M^+), 431 (100). Anal. calc. for $\text{C}_{22}\text{H}_{12}\text{Cl}_4\text{N}_4\text{Zn}_2$: C 43.7, H 2.0, N 9.3; found: C 43.5, H 2.1, N 9.4.

The preparations of the Ru^{II} complexes have been described in [6].

We thank the University of Dicle, Diyarbakir, Turkey for support of Akin Baysal during leave of absence, the EPSRC Mass Spectrometry Service at Swansea (Dr. J. A. Ballantine), and our colleagues at Canterbury, Dr. R. E. Benfield, Dr. J. A. Creighton, Mr. A. J. Fassam, Dr. D. O. Smith and Dr. M. J. Went for their help.

REFERENCES

- [1] V. Balzani and L. D. Cola, 'Transition Metals in Supramolecular Chemistry', Kluwer, Dordrecht, 1992; J. M. Lehn, 'Supramolecular Chemistry', VCH, Weinheim, 1995.
- [2] H. A. Goodwin, F. Lions, *J. Am. Chem. Soc.* **1959**, *81*, 6415.
- [3] S. Campagna, G. Denti, S. Serroni, A. Juris, M. Venturi, V. Ricevuto, V. Balzani, *Chem. Eur. J.* **1995**, *1*, 211; M. B. Ferrari, G. G. Fava, G. Pelosi, G. Predieri, C. Vignali, G. Denti, S. Serroni, *Inorg. Chim. Acta* **1998**, *275–276*, 320.
- [4] G. J. Leigh, *Chem. Brit.* **1993**, 574.
- [5] D. D. Bly, M. G. Mellon, *J. Org. Chem.*, **1962**, *27*, 2945; M. Hunziker, A. Ludi, *J. Am. Chem. Soc.* **1977**, *99*, 7370.
- [6] M. Riklin, A. von Zelewsky, *Helv. Chim. Acta* **1996**, *79*, 2176.
- [7] P. N. W. Baxter, J. A. Connor, J. D. Wallis, D. C. Povey, A. K. Powell, *J. Chem. Soc., Perkin Trans. 1* **1992**, 1601.
- [8] G. R. Newkome, J. M. Roper, *J. Org. Chem.* **1979**, *44*, 502.
- [9] C. Graebe, *Ber. Dtsch. Chem. Ges.* **1892**, *25*, 3146; J. Thiele, A. Wandscheidt, *Ann. Chem.* **1910**, *376*, 269.
- [10] J. S. Lee, S. C. Nyburg, *Acta Crystallogr., Sect. C* **1985**, *41*, 560.
- [11] J. Druey, P. Schmidt, *Helv. Chim. Acta* **1950**, *33*, 1080.
- [12] K. Kloc, J. Mlochowski, Z. Szulc, *Heterocycles* **1978**, *9*, 849.
- [13] C. Djerassi, *Chem. Rev.* **1948**, *48*, 271; R. C. Fuson, H. D. Porter, *J. Am. Chem. Soc.* **1948**, *70*, 895.
- [14] H. C. Brown, I. Moritani, *J. Am. Chem. Soc.* **1953**, *75*, 4112.
- [15] E. A. Braude, A. G. Brook, R. P. Linstead, *J. Chem. Soc.* **1954**, 3569; P. P. Fu, R. G. Harvey, *Chem. Rev.* **1978**, *78*, 317.
- [16] B. M. Trost, D. R. Brittelli, *J. Org. Chem.* **1967**, *32*, 2620.
- [17] Y. Cohen, J. Klein, M. Rabinovitz, *J. Chem. Soc., Chem. Commun.* **1986**, 1071.
- [18] L. Angeloni, S. Panerai, G. Sbrana, *J. Raman Spectros.* **1982**, *12*, 30.
- [19] J. Fabian, R. Zahradnik, *Angew. Chem., Int. Ed.* **1989**, *28*, 677.
- [20] E. van der Donckt, P. Toussaint, C. van Vooren, A van Sinoy, *J. Chem. Soc. Faraday Trans. 1* **1976**, *72*, 2301.
- [21] M. Otero, E. Roman, E. Samuel, D. Gourier, *J. Electroanal. Chem.* **1992**, *325*, 143.
- [22] I. C. Lewis, L. S. Singer, *J. Chem. Phys.* **1966**, *44*, 2082; J. C. Chippendale, P. S. Gill, E. Warhurst, *Trans. Faraday Soc.* **1967**, *63*, 1088.
- [23] E. L. Eliel, S. H. Wilen, L. N. Mander, 'Stereochemistry of Organic Compounds', Wiley, New York, 1994.
- [24] Y. Tanaka, European Patent appl., 0861840; *Chem. Ind. (London)* **1998**, 726.
- [25] D. A. Dougherty, F. M. Lort, K. Mislow, J. F. Blount, *Tetrahedron* **1978**, *34*, 1301.
- [26] M. H. Chisholm, J. C. Huffman, I. P. Rothwell, P. G. Bradley, N. Kress, W. H. Woodruff, *J. Am. Chem. Soc.* **1981**, *103*, 4945.
- [27] R. A. Klein, P. Witte, R. van Belzen, J. Fraanje, K. Goubitz, M. Numan, H. Schenk, J. M. Ernsting, C. J. Elsevier, *Eur. J. Inorg. Chem.* **1998**, 319.
- [28] R. E. Gerkin, A. P. Lundstedt, W. J. Reppart, *Acta Crystallogr., Sect. C* **1984**, *40*, 1892.
- [29] A. A. Schilt, 'Analytical Applications of 1,10-Phenanthroline and Related Compounds', Pergamon, Oxford, 1969.
- [30] J. S. Lee, I. Y. Chen, *J. Chinese Chem. Soc.* **1989**, *36*, 123.
- [31] K. D. Truong, A. D. Bandrauk, *Can. J. Chem.* **1977**, *55*, 3712; L. Angeloni, G. Sbrana, *J. Raman Spectros.* **1983**, *14*, 380.
- [32] Z. R. Grabowski, K. Rotkiewicz, A. Siemiarczuk, D. J. Cowley, W. Baumann, *Nouv. J. Chim.* **1979**, *3*, 443; C. A. Hunter, J. K. M. Sanders, *J. Am. Chem. Soc.* **1990**, *112*, 5525.
- [33] S. Flandrois, D. Chasseau, *Acta Crystallogr., Sect. B* **1977**, *33*, 2744.
- [34] L. J. Henderson, F. R. Fronczek, W. R. Cherry, *J. Am. Chem. Soc.* **1984**, *106*, 5876.
- [35] SHELXTL, PC version 5.03, *Siemens Analytical Instruments Inc.*, Madison WI, 1994.

Received June 26, 1999